Journal of Aeronautics & Aerospace Engineering

Xiakai et al., J Aeronaut Aerospace Eng 2012, 1:1
DOI: 10.4172/2168-9792.1000101

Research Article Open Access

Research on Heading Sensitive Drift Behavior of Inertial Platform System under Long-term Storage Condition

Huang Xiakai*, Chen Yunxia and Kang Rui

School of Reliability and System Engineering, Beihang University, Beijing 100191, China

Abstract

The heading sensitive drift of inertial platform system changes with the degradation of components' performance and the coupling characteristics under long-term storage conditions. Such heading sensitive drift is different from the drift under working conditions, and it is difficult to analyze its stability for allocating resources for the calibration and maintenance in engineering application. In this paper, firstly the theory and expression of heading sensitive drift caused by servo loop zero and structure disturbing torque was presented and derived. Secondly, the drift characteristic of influence parameters was analyzed thoroughly based on the expression, and the integrated behavioral model of heading sensitive drift under servo loop zero and disturbing torque influence was concluded. And then, the long-time drift characteristic, acceleration performance and stability of heading sensitive drift behavior were analyzed with actual storage condition profile. The results indicate that heading sensitive drift on the X, Y and Z axis has the similar long-term drift characteristics without acceleration response, which is different from the response characteristic in actual use and therefore has great significance for allocating resources for the calibration and maintenance in inertial platform system.

Key words: Long-term storage; Heading sensitive drift behavioral; Servo loop zero; Structure disturbing torque

Introduction

Heading sensitive drift mainly refers to the phenomenon of output of Gyro drifts along with the heading altitude change of inertial platform system, and its value is more than ten times or even scores of times of Gyro precision level with unpredictable drift status, which is a difficult issue for the research of inertial platform system precision nowadays [1-3].

The influence mechanism of heading sensitive drift is complicated and inter-correlated, and its influencing factors are generally summed up into the following four: servo loop zero and structure disturbing torque, vibration, temperature and magnetic influence. Currently, researches in this regard mainly focus on the transient response of heading sensitive drift, and compensation design for the using precision of heading sensitive drift is conducted accordingly [4-7].

For the missile inertial platform system which has the characteristic of long-term storage and one time usage, many factors including bearing stiffness changing, materials creep, lubrication damping degradation and so on have great influence on the heading sensitive drift behavior under long-term storage conditions, and as their influence mechanism is complicated and inter-correlated [8-10], it brings great difficulty for the calibration and maintenance of the inertial platform system heading sensitive drift. Therefore, the research of inertial platform system heading sensitive drift storage stability is very significant for allocating resources for the calibration and maintenance.

In the paper, the influence principle of servo loop zero and structure disturbing torque is discussed, and expression of heading sensitive drift is derived from the above influence principle theory. Secondly, the drift characteristic of parameter in the expression is analyzed by comprehensive analysis and experiment measurement, and then integrated behavioral model of heading sensitive drift under servo loop zero and disturbing torque influence is concluded. Ultimately, the long-time drift characteristic, acceleration performance and stability of heading sensitive drift behavior were analyzed with actual storage condition profile. The results indicate that heading sensitive drift on the X, Y and Z axis has the similar long-term drift characteristics without acceleration response, which is different from the response characteristic in actual use and therefore has great significance for allocating resources for the calibration and maintenance in inertial platform system.

The Principle of Heading Sensitive Drift Caused by Servo Loop Zero and Structure Disturbing Torque

Research object

Figure 1 is the frame structure of inertial platform system - the research object of this paper, which is mainly composed of azimuth ring,

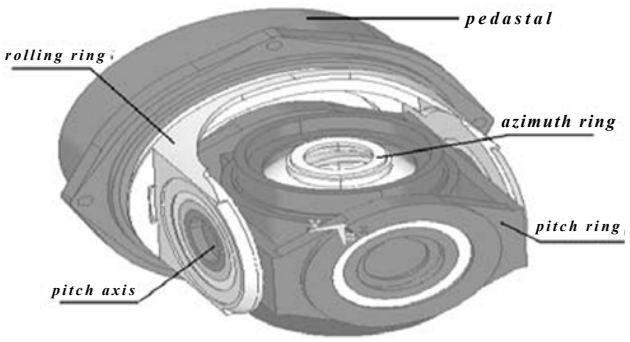

Figure 1: Frame structure of inertial platform system.

***Corresponding author:** Huang Xiakai, School of Reliability and System Engineering, Beihang University, Beijing 100191 China, E-mail: huangxiaokai1986@126.com

Received March 06, 2012; **Accepted** May 30, 2012; **Published** May 02, 2012

Citation: Xiakai H, Yunxia C, Rui K (2012) Research on Heading Sensitive Drift Behavior of Inertial Platform System under Long-term Storage Condition. J Aeronaut Aerospace Eng 1:101. doi:10.4172/2168-9792.1000101

pitch ring, rolling ring and other connection structure, and provides the pitch angle, the roll angle and the azimuth angle measurements needed by missile altitude control for the device through altitude angle sensor on the gimbal axis [11].

Under the long-term storage conditions, servo loop zero and structure disturbing torque of inertial platform system in Figure 1 will change with the materials creep or heading altitude angle drift, which makes the gyros output additional angle related to the heading altitude angle drift [12].

The principle of heading sensitive drift caused by servo loop zero and structure disturbing torque

Inertial platform system isolate the angle movement by the three servo loops of the azimuth ring, the pitch ring and rolling ring, so as to maintain the stability and tracking of the inertial platform structure. With comprehensive analysis, the detailed block diagram of the rolling ring and pitch ring's servo loops of vertical gyros is shown in Figure 2, and the detailed block diagram of the servo loop and its self-locking loop of traverse gyro is shown in Figure 3 [6,7,13].

It can be concluded from Figure 2 and Figure 3 that the heading sensitive drift caused by servo loop zero is as follow:

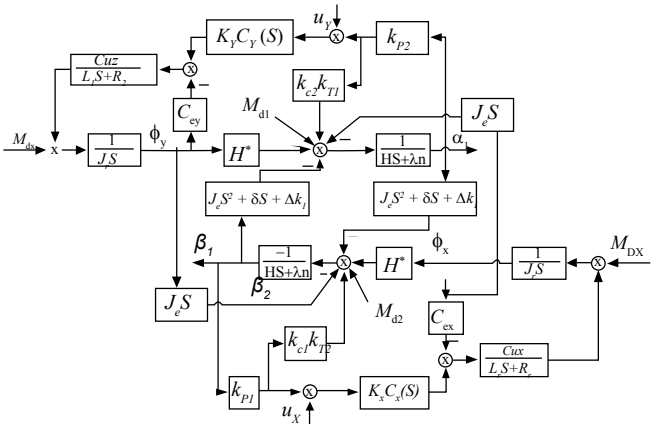

Figure 2: Detailed block diagram of the servo loop of vertical gyros rolling ring and pitch ring.

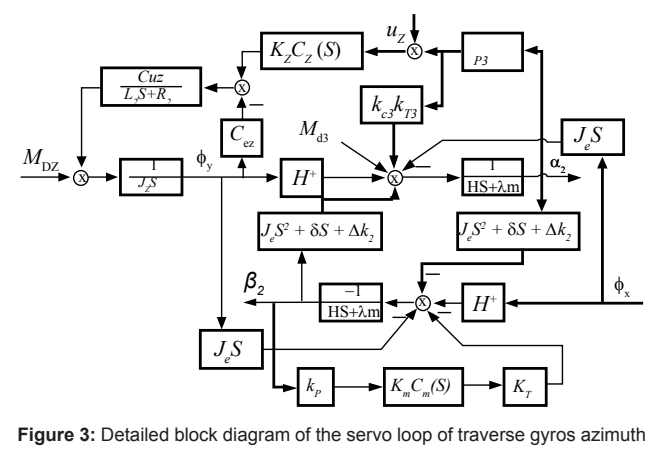

Figure 3: Detailed block diagram of the servo loop of traverse gyros azimuth ring and its self-locking loop.

$$\begin{aligned}\omega_{PX} &= \frac{1}{\tau_1 k_{P2} K_1}(u_x\cos\psi - u_Y\sin\psi) - \frac{\Delta k_1}{H k_{P2} K_1}(u_X\sin\psi + u_Y\cos\psi)\\ \omega_{PY} &= \frac{1}{\tau_1 k_{P2} K_1}(u_x\sin\psi + u_Y\cos\psi) - \frac{\Delta k_1}{H k_{P1} K_1}(u_X\cos\psi - u_Y\sin\psi)\\ \omega_{PZ} &= \frac{u_Z}{\tau_2 k_{P3} K_1} - \frac{\Delta k_2}{H}\beta_2\end{aligned} \quad (1)$$

The heading sensitive drift caused by structure disturbing torque is as follow:

$$\begin{aligned}\omega'_{PX} &= \frac{1}{\tau_1 S_0}(M_{DX}\cos\psi - M_{DY}\sin\psi) - \frac{\Delta k_1}{H S_0}(M_{DX}\sin\psi + M_{DY}\cos\psi)\\ \omega'_{PY} &= \frac{1}{\tau_1 S_0}(M_{DX}\sin\psi + M_{DY}\cos\psi) - \frac{\Delta k_1}{H S_0}(M_{DX}\cos\psi - M_{DY}\sin\psi)\\ \omega'_{PZ} &= \frac{u_Z}{\tau_2 k_{P3} K_1} - \frac{\Delta k_2}{H}\beta_2\end{aligned} \quad (2)$$

Where, τ1, τ2 are the time constants of vertical gyro and traverse gyro; K1 is the scale factor of the preamplifier, H is the gyro angular momentum; S0 is the stiffness coefficient of the servo loop; M_{DX}, M_{DY}, M_{DZ} are the structure disturbing torque from the pitch axis, rolling axis and azimuth axis of the inertial platform system respectively; u_X, u_Y, u_Z are the servo loop zero from pitch servo loop, rolling servo loop and azimuth servo loop of the inertial platform system respectively; k_{P1}, k_{P2}, k_{P3} are the sensor scale coefficients of vertical gyro's X axis and Y axis and traverse gyro's Y axis; β_2 is the drift angle of traverse gyro rotor rolling around the Y axis and X axis, Δk_1, Δk_2 are the residual elastic coefficients of vertical gyro and traverse gyro respectively; λ_1, λ_2 are the orthogonal damping elasticity coefficients of vertical gyro and traverse gyro; ψ is the heading angle.

Drift Behavioral Model of Inertial Platform System

Engineering experience has shown that servo loop zero mainly refers to AC interference in demodulator input terminal and input zero of DC amplifier, both of which can be analyzed by converting into the input of demodulator, meanwhile, the disturbing torque taking effect on the gimbal axis mainly refers to the bearing friction torque [1,14]. Therefore, this section deeply analyzed the creep mechanism and behavior characteristic of demodulator input zero and bearing friction torque, analyzed the behavioral characteristics of model parameters in equations (1) and (2), and then comprehensively derived the heading sensitive drift behavioral model of inertial platform system.

Drift behavior of servo loop zero

In inertial platform system, the drift mechanism of servo loop zero in servo loop shown in figure 4(use the pitch servo loop and rolling servo loop for examples).

Wang Fang et al. [14] pointed out that servo loop zero will change with temperature and u_x, u_y, u_z mainly refer to 19.2 KHz AC interferences in demodulator input terminal and input zero of DC amplifier, which are analog circuit parameters and their performance depends on the creep characteristic of the resistor, the capacitor and the amplifier.

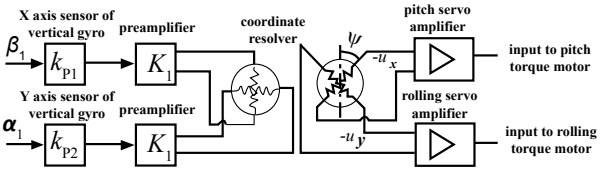

Figure 4: The produce mechanism of servo loop zero.

parameters	value
average speed n(r/min)	5
bearing's inner diameter d/mm	60
bearing's outer diameter D/mm	95
axial load N	150
Radial load N	180
f_0	6
f_1	5×10^{-4}

Table 1: Parameters of certain sealed spherical roller bearing

The paper analyzed the degradation features of preamplifier in servo loop by experiment, and then got the drift behavioral model of servo loop zero with the initial value $u_X = u_Y = u_Z = 10mV = 0.01V$ as follow:

$$u_X = u_Y = u_Z = 0.01\times(17.4132 - 1.04775\times10^{-4}\times t - 0.00139899\times T + 2.31568\times10^{-9}\times t^2 + 2.35779\times10^{-8}\times T^2 + 2.9888\times10^{-9}\times t\times T) \quad (3)$$

Drift behavior of bearing friction torque

Bearing friction torque means all kinds of damping torque related to bearing rotating, which not only involves bearing structure, dimensions, materials, heat treatment performance, but is also influenced by the working load, lubrication situation and environment, and all those factors interact and interfere with each other, which makes the research even more complicated [10-12].

Bearing friction torque is a hot research issue currently. Its computational method can be divided into two categories, i.e., quasi static analytical method based on Herz elastic contact theory and engineering experience formula based on dynamical friction theory [15-17]. Under the long-term storage conditions, due to factors like the combat readiness or test calibration, the bearing friction torque in certain inertial platform system is featured by dynamical friction. Therefore, it can be calculated by engineering experience formula, which means dividing the bearing friction torque into two parts according to whether it is caused by working load or not, and the expression is as follows [16]:

$$M = M_0 + M_1 = 10^{-7} f_0 (vn)^{2/3} D_0^3 + \mu_1 f_1 F D_0 / 2 \quad (4)$$

Where: M_0 is the bearing friction torque without loads ($N\bullet mm$); M_1 is the bearing friction torque caused by loads ($N\bullet mm$); f_0 means the bushes type and lubrication type; v is the lubrication coefficient of lubricant base oil under the operating temperature (mm^2/s); n is the bearing speed (r/ min); $D_0 = (d+D)/2$ is the bearing average diameter (mm), among d is the bearing's inner diameter, D is the bearing's outer diameter; μ is the friction coefficient; f1 is the factor reflecting the load direction; F is the bearing load (N), , F_r is the bearing's radial load (N) $F = sqrt(F_r^2 + F_a^2)$, F_a is the bearing's axial load (N).

The parameter data in Table 1 is the roller bearing structure parameter value used in certain inertial platform system.

Under the long-term storage conditions, lubrication coefficient and friction coefficient have the creep feature, which exert a tremendous influence on the bearing friction torque.

Creep law of lubrication coefficient: Under the storage condition, bearing in inertial platform system cannot add any extra lubricant, but meanwhile it has to be made sure that there is no lubricant starvation or lubricant accumulation. Therefore, the creep will occur to the lubricant coefficient under the impact of factors like time or temperature during the storage, which will result in changes of the bearing friction torque.

Based on Hagen-Poiseuille's law of capillary viscosity measurements, we obtained the lubrication coefficient creep model of certain lubricating oil within different storage temperature rang (20°C~70°C) along with the time shown as follow:

$$v = 0.05\times10^{-3.28+0.016T}\times(0.835\times\log t + 2.47) \quad (5)$$

Creep law of friction coefficient: The combined influence of the over surplus assembly, micro components on the material surface and the surface roughness in bearing structure makes the bearing friction coefficient drift mechanism complicated and difficult to figure out.

With the axial and radial loads as shown in Table 1, the creep model of roller bearing friction coefficient of certain inertial platform system drift along with temperature and time can be concluded as follow:

$$\mu = 0.0135\ln(t) + 0.1273 \quad (6)$$

Combine equation (4), (5), (6) and the data in Table 1, the drift mechanism model of the bearing friction coefficient can be concluded as follow:

$$\begin{aligned} M &= 10^{-7} f_0 (vn)^{2/3} D_0^3 + (\mu f_1 F D_0)/2 \\ &= 10^{-7}\times6(0.05\times10^{-3.28+0.016T}\times(0.835\times\log t + 2.47)\times30)^{2/3}\times77.5^3 \\ &+\left\{(0.0135\ln t + 0.1273)\times5\times10^{-4}\times\sqrt{150^2+180^2}\times77.5\right\}/2 \\ &= 0.3659743\times\left\{10^{-3.28+0.016T}\times(0.835\times\log t + 2.47)\right\}^{2/3} \\ &+0.0613\ln t + 0.5779 \end{aligned} \quad (7)$$

Analysis of heading sensitive drift model parameter drift behavior

Heading sensitive drift expression caused by servo loop zero and structure disturbing torque is related to the preamplifier scale factor K_1, sensor scale factors kp_1,kp2, gyro angular momentum H, gyro time constant τ, residual elastic coefficient Δk, drift angle of traverse gyro rotor Y axis and X axis β_2 and servo loop stiffness S_0,the paper studied there parameters respectively.

Scale factor of preamplifier: The degradation rule of the preamplifier is similar to that of the resistor and capacitor, and according to the acceleration characteristic of analog electronic products, we choose the Arrhenius as the preamplifier behavior model, which suitable for mainly affected by temperature situation [18].

Through the experiment analysis of preamplifier's key resistor drift characteristic, we can get the preamplifier behavior model with the initial value $K_1 = 50$ as follow:

$$K_1 = 50\times(17.4132 - 1.04775\times10^{-4}\times t - 0.00139899\times T + 2.31568\times10^{-9}\times t^2 + 2.35779\times10^{-8}\times T2 + 2.9888\times10^{-9}\times t\times T) \quad (8)$$

Scale factor of sensor: Sensor, which takes many forms, is a measuring system composed of sensitive components and measuring circuit, and the sensor used in dynamically tuned gyro is variable reluctance inductive sensor [19].

The derivation expression of variable reluctance inductive sensor is as follow [13]:

$$Kp = \dot{U}/(2\delta_0) \quad (9)$$

Where, K_p is the scale factor of sensor, δ_0 is the initial clearance between iron core and magnetic conductance ring, $\Delta\delta = ra$, r is the center diameter of the sensor's iron core, and a is the rotating angle of gyro rotor.

Engineering experience has proved that the drift of sensor scale fac-

tor is mainly caused by the clearance change between iron core and magnetic conductance ring, and also the center diameter parameter drift of the sensor's iron core, Such change or drift is mainly influenced by the thermal expansion coefficient under the working of temperature, however, the thermal expansion coefficient does not have temperature acceleration characteristic. Therefore, constant design value of the sensor's scale factor is set at $k_{P1}=k_{P2}$=2.5mV/arc minute.

Gyro angular momentum: The expression of gyro angular momentum is as follows [13]:

$$H=Jz\omega \quad (10)$$

Where, J_Z is the polar axis rotational inertia of the gyroscope rotor; $\omega = \pi f/30$ is the rotation angular speed of the gyroscope rotor, rad/s; f is the speed of the gyroscope rotor, r/min.

We can conclude from the above that gyro angular momentum mainly depends on its design value and is not influenced by the temperature or the time. Therefore, we set the initial value at H = 74.088kg•m^2/h here in this paper.

Gyro time constant: The computational expression of gyro time constant is as follow [13]:

$$\tau = H / \lambda = J_z / \left(\xi + \delta_1\right) \quad (11)$$

Where, J_Z is the polar axis rotational inertia of the gyroscope rotor, ξ is the damping coefficient of the rotor gas, δ_1 is the internal friction damping coefficient of the flexible hinge, and λ is the orthogonal elastic damping coefficient.

From the description of the above parameters, it can easily concluded that gyro time constant is mainly influenced by material damping, and the we can use the drift rule of material's damping coefficient degradation to reflect the degradation characteristic of the gyro time constant. Based on the concept of equivalent viscous damping, the paper converts the gyro damping into viscous damping (the conversion method is to deem that viscous damping consumes the same energy with other viscous damping in a vibration period), and take it as the acceleration coefficient of the gyro time constant. Ultimately, the behavior model of gyro time constant with an initial value τ_1 = 1/60h of in certain inertial platform system is as follow:

$$\tau_1 = \tau_2 = 0.015078 \times (+0.421652122 \times 10^{-8} \times e^{19.35-\frac{18.51}{T}}) \times \ln t \quad (12)$$

Residual elastic coefficient: The definition of residual elastic coefficient is as follow [13]:

$$\Delta k = K_0 = (a+b-c)N^2/2 \quad (13)$$

Where, $K_0=(a+b-c)N^2/2$ is the rigidity elastic coefficient of gyro, a, b and c are the rotational inertia around X axis Y axis and Z axis of middle gimbals ring respectively, N is spin velocity of gyro, and N_0 is the tuning speed of gyro under the tuned state.

Generally, after the flexible support structure parameters are determined, the parameters that can be adjusted are only the rotational inertia a, b, and c and rotating speed N. Therefore, the drift of residual elastic coefficient is only related to the stiffness characteristic of bearing material. The paper makes experimental analysis of the material stiffness characteristic of dynamically tuned gyro and concludes the drift behavior model of residual elastic coefficient as follow:

$$\Delta k_1 = \frac{\pi}{360} \times 10^{-5} \times \frac{3 \times 10^8 - \frac{1}{\sqrt{2.3275 \times 10^{-16} t \exp(-26.6/8.31T)}}}{1.75 \times 10^{11}} \quad (14)$$

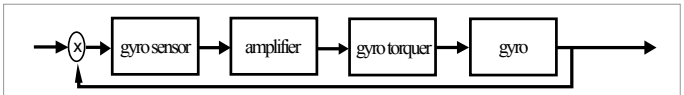

Figure 5: The functional block diagram of gyro X axis works on servo loop.

Drift angle of azimuth gyro around X axis: The X axis of azimuth gyro connected to inertial platform structure by the self-locking loop, and thus β_2 only depends on the loop zero and its output of the self-locking loop, which do not change with heading angle. The functional block diagram of gyro X axis' work on the servo loop is shown in Figure 5 [13].

Gyro sensor converts the rotate angle of the X axis into electrical signal and transmits it into the lock-in amplifier, which then supplies the gyro torque with current proportionate to the electrical signal, and finally the gyro torque produces moment to enable the rotation of gyro until the gyro H axis is brought to zero.

Therefore, the behavior characteristic of the drift angle of azimuth gyro around X axis is the same with the servo loop zero in terms of behavior. The drift behavior model of the drift angle of the azimuth gyro around X axis with an initial value β_2=1.5×10-^{6}rad = (270/π)×10-^{6}°can be concluded according to equation (3) below:

$$\beta 2 = (270/\pi)\times 10\text{-}^6 \times (17.4132 - 1.04775 \times 10\text{-}^4 \times t - 0.00139899 \times T + 2.31568 \times 10\text{-}^9 \times t2 + 2.35779 \times 10\text{-}^8 \times T^2 + 2.9888 \times 10\text{-}^9 \times t \times T) \quad (15)$$

Stiffness of servo loop: The principle of servo loop stiffness is as follow [20]:

$$S_\theta(s) = \frac{1}{\varphi(s)} = \frac{M_D(s)}{\theta(s)} = Js^2 + K_g K_a' K_m F(s)/R \quad (16)$$

Where, $K_g=H/C$, and C is the viscous damping coefficient, K_m is the motor torque coefficient, R is the total resistance of torque motor, $K_a'F(s)$ is the transfer function of servo amplifier, K_a' is the total magnification of servo amplifier, F(s) is the network transfer function, and J is the total moment inertia of the torque motor around output shaft.

From the above analysis, it can be seen that the acceleration of the servo loop stiffness depends on the performance of the servo loop, and thus has the same degradation characteristic with the servo loop. By referring to equation (3) above, the drift behavior model of servo loop stiffness with an initial value of $S_0 = 5\times10^7 g\bullet cm/rad = (50\pi/18) kg\bullet m/^\circ$ can be concluded as follows:

$$S_0 = ((50\pi)/18) \times (17.4132 - 1.04775 \times 10^{-4} \times t - 0.00139899 \times T + 2.31568 \times 10^{-9} \times t^2 + 2.35779 \times 10^{-8} \times T^2 + 2.9888 \times 10^{-9} \times t \times T) \quad (17)$$

Drift behavioral model for the heading sensitive drift of inertial platform system

Inserting equations (3) ~ (17) into equation (1) and (2) , i.e. heading sensitive drift caused by servo loop zero and structure disturbing torque respectively, we can easily get the synthetical drift behavioral model with $M_{X0}=M_{Y0}=M_{z0}$ and unified parameters unit. In order to analyze the model in a more vivid and effective way, this paper applies the response surface identification method to rewrite the mechanism equation (1) and (2), which results in equation (18) as below:

$\omega_X = \omega_{PX} + \omega'_{PX}$ = 0.013528735853104 - 1.0606312285 x 10^{-5}g - 5.537104156 x 10^{-6} T - 4.23727461 x 10^{-7} t +1.759374 x 10^{-9} g x T + 7.6329 X 10^{-11}g x t +2.6142 x 10^{-11} T x t +3.84714339 x 10^{-7} g^2 + 5.438001 x 10^{-9} T^2 + 1.2679 x10^{-11} t^2 + 0.901256402152763 - 8.33169068108 x 10^{-4}g - 4.40627696664 x 10^{-4} T + 5.279128685 X 10^{-6} t +1.47853436 x 10^{-7} g

Drift time/ year		1	2	3	4	5	6	7	8	9	10
X axis heading sensitive drift(°/h)	20°C	0.0182546	0.0178035	0.0175922	0.0174423	0.0173068	0.0171677	0.0170170	0.0168512	0.0166694	0.0164718
	40°C	0.0181831	0.0177338	0.0175234	0.0173741	0.0172391	0.0171005	0.0169503	0.0167851	0.0166039	0.0164071
	60°C	0.0181206	0.0176730	0.0174633	0173145	0.0171799	0.0170418	0.0168920	0.0167274	0.0165468	0.0163505
	80°C	0.0180657	0.0176195	0.0174104	0.0172620	0.0171279	0.0169901	0.0168408	0.0166766	0.0164964	0.0163007
	100°C	0.0180170	0.0175720	0.0173636	0.0172156	0.0170818	0.0169443	0.0167953	0.0166315	0.0164518	0.0162565
Y axis heading sensitive drift(°/h)	20°C	0.0182546	0.0178036	0.0175923	0.0174424	0.0173069	0.0171678	0.0170171	0.0168513	0.0166695	0.0164719
	40°C	0.0181832	0.0177339	0.0175235	0.0173742	0.0172392	0.0171006	0.0169504	0.0167852	0.0166041	0.0164072
	60°C	0.0181207	0.0176731	0.0174634	0.0173146	0.0171801	0.0170419	0.0168922	0.0167275	0.0164965	0.0163008
	80°C	0.0180658	0.0176196	0.0174105	0.0172622	0.0171280	0.0169902	0.0168409	0.0166767	0.0164965	0.0163008
	100°C	0.0180171	0.0175722	0.0173637	0.0172157	0.0170819	0.0169444	0.0167954	0.0166316	0.0164519	0.0162566
Z axis heading sensitive drift(°/h)	20°C	0.0182546	0.0178035	0.0175922	0.0174423	0.0173069	0.0171677	0.0170170	0.0168513	0.0166694	0.0164719
	40°C	0.0181831	0.0177339	0.0175234	0.0173741	0.0172391	0.0171005	0.0169503	0.0167852	0.0166040	0.0164071
	60°C	0.0181207	0.0176731	0.0174633	0.0173145	0.0171800	0.0170418	0.0168921	0.0167274	0.0165468	0.0163505
	80°C	0.0180657	0.0176195	0.0174105	0.0172621	0.0171279	0.0169901	0.0168408	0.0166766	0.0164965	0.0163007
	100°C	0.0180170	0.0175721	0.0173636	0.0172156	0.0170818	0.0169443	0.0167954	0.0166315	0.0164518	0.0162565

Table 2: Behavioral data of inertial platform system heading sensitive drift in storage condition.

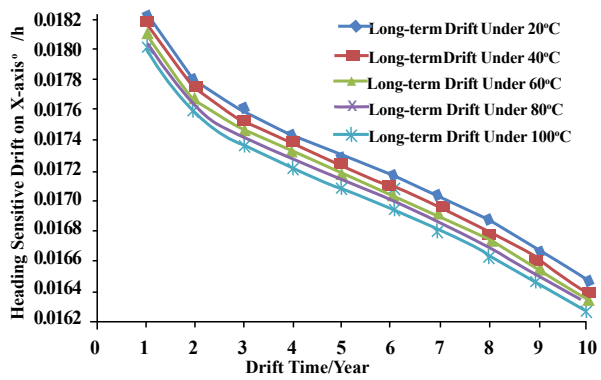

Figure 6: Drift law of inertial platform system heading sensitive drift on X-axis.

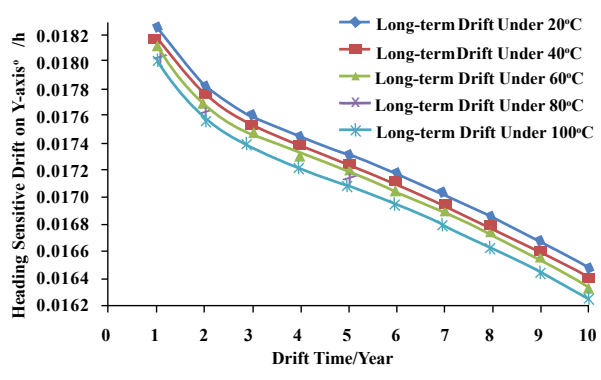

Figure 7: Drift law of inertial platform system heading sensitive drift on Y-axis.

$x\ T - 1.651471 \times 10^{-9}\ g\ x\ t - 5.43285 \times 10^{-10}\ T\ x\ t + 3.3436136318 \times 10^{-5}\ g^2 + 4.70814861 \times 10^{-7}\ T^2 - 8.9493 \times 10^{-11}\ t^2$

$\omega_Y - \omega_{PY} + \omega'_{PY} - 0.013527824455615 - 1.060631872 \times 10^{-5}\ g - 5.532447054 \times 10^{-6}\ T - 4.23704875 \times 10^{-7}\ t + 1.759392 \times 10^{-9}\ g\ x\ T + 7.6329 \times 10^{-11}\ g\ x\ t + 2.6095 \times 10^{-11}\ T\ x\ t + 3.84714273 \times 10^{-7}\ g^2 + 5.432393 \times 10^{-9}\ T^2 + 1.2678 \times 10^{-11}\ t^2 + 0.901184717331631 - 8.3316907565 \times 10^{-4}\ g - 4.4025611517 \times 10^{-4}\ T + 5.280729664 \times 10^{-6}\ t + 1.47853481 \times 10^{-7}\ g\ x\ T - 1.651471 \times 10^{-9}\ g\ x\ t - 5.46192 \times 10^{-10}\ T\ x\ t + 3.3436136301 \times 10^{-5}\ g^2 + 4.70355533 \times 10^{-7}\ T^2 + 8.9514 \times 10^{-11}\ t^2$

$\omega_Z - \omega_{PZ} + \omega'_{PZ} - 0.013528314450239 - 1.0606338982 \times 10^{-5}\ g - 5.534950528 \times 10^{-6}\ T - 4.23717017 \times 10^{-7}\ t + 1.759454 \times 10^{-9}\ g\ x\ T + 7.6329 \times 10^{-11}\ g\ x\ t + 2.612x\ 10^{-11}\ T\ x\ t + 3.84714404 \times 10^{-7}\ g^2 + 5.435407 \times 10^{-9}\ T^2 + 1.2679\ X\ 10^{-11}\ t^2 + 0.901220595325726 - 8.33169101491 \times 10^{-4}\ g - 4.40442088735 \times 10^{-4}\ T + 5.279928327 \times 10^{-6}\ t + 1.47853563 \times 10^{-7}\ g\ x\ T - 1.651471 \times 10^{-9}\ g\ x\ t - 5.44737 \times 10^{-10}\ T\ x\ t + 3.3436136534 \times 10^{-5}\ g^2 + 4.70585418 \times 10^{-7}\ T^2 - 8.9503 \times 10\text{-}^{11}\ t^2$

Analysis of Inertial Platform System Heading Sensitive Drift Behavior under Storage Condition

Simulating the equation (18) by Matlab with the heading angle set at zero, the paper gets the data of inertial platform system heading drift in ten years under different temperature and the results are shown in Table 2.

Fitting the data in Table 2, we can get the drift curve shown as Figure 6-8.

Long-term drift characteristic analysis: From Figure 6-8, it can be

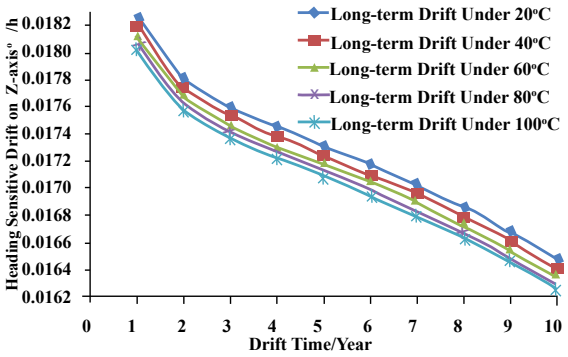

Figure 8: Drift law of inertial platform system heading sensitive drift on Z-axis.

Storage period	X axis stability	Y axis stability	Y axis stability
1 year	0.14304378	0.142997679	0.143023471
2 years	0.143492198	0.143446075	0.143471879
3 years	0.143702901	0.14365677	0.143682578
4 years	0.14385262	0.143806484	0.143832295
5 years	0.143988075	0.143941935	0.143967748
6 years	0.143993762	0.143946623	0.143972435
7 years	0.144002423	0.143956285	0.143982097
8 years	0.14401845	0.143972313	0.143998125
9 years	0.144034531	0.143988394	0.144014205
10 years	0.144050275	0.144004138	0.144029949

Table 3: Analysis result of storage stability of inertial platform system heading sensitive drift.

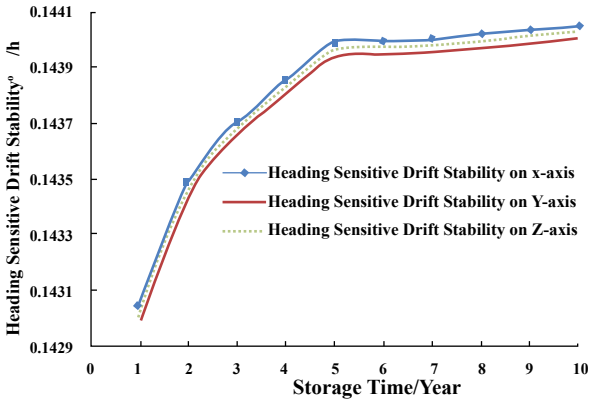

Figure 9: drift curve of heading sensitive drift stability.

easily found that heading sensitive drift has similar drift characteristic on X, Y and Z axis under long-term storage conditions, and this phenomenon is different from that under the operating conditions, as under operating conditions, drift on X axis and Y axis is larger than that on Z axis [1].

Acceleration feature analysis: From Figure 8-10, it can be easily found that the temperature change has little influence on the heading sensitive drift, but the drift is obvious under the long-term working of temperature, which means the temperature has no acceleration feature with the heading sensitive drift caused by servo loop zero and structure disturbing torque.

Storage stability analysis: The average storage temperature in the warehouse is 20°C, a storage cycle is to calibrate the heading sensitive drift every 12 months, the calibration temperature is 70°C, and the time of calibration is 48 hours. The paper simulates the accumulative drift value after every cycle and analyzes its storage stability with the result shown in Table 3.

Fit the stability data on X axis, Y axis and Z axis in Table 3 and we can get the curve drawn as Figure 9.

From Table 3 and Figure 9, we can find that without regard to the influence of vibration, temperature and magnetic field, the storage stability of heading sensitive drift caused by servo loop zero and structure disturbing torque can meet the requirement of the stability for one year in current engineering, that is, 0.2°C/h (which means the biggest drift difference ≤ 0.2°C/h), however, the stability value still contributes a lot to the whole drift. Therefore, the optimization of resource calibration and maintenance is still of great concern for the heading sensitive drift.

Conclusion

In this paper, the principle of inertial platform system heading sensitive drift caused by servo loop zero and structure disturbing torque is comprehensively analyzed and discussed and the parameters characteristic of heading sensitive drift behavioral model is derived with experiment measurement. Finally, the behavioral model of heading sensitive drift is summarized and the storage stability is analyzed under actual storage environmental profile. The research approach and conclusion are meaningful not only to theoretical research but also engineering application. The major contribution and innovative points are as follow:

(1) The bearing stiffness drift, material creep and lubrication damping characteristics are considered in the heading sensitive drift research under long-term storage condition for the first time, which has provided theoretical support for the heading sensitive drift behavioral analysis of inertial platform system with the feature of "long-term storage and one time using".

(2) Through deep analysis of the mechanism of bearing friction torque and behavioral of heading sensitive drift model parameters, the paper has deduced the behavioral model of inertial platform system's heading sensitive drift, and has vividly presented the long-term drift behavioral performance along with temperature and time by system identification method.

(3) Through the analysis of heading sensitive drift's storage behavioral, the paper concludes that the heading sensitive drift caused by servo loop zero and structure disturbing torque does not have acceleration feature, and the stability drift value, while meeting the requirement of long-term stability, still contribute a lot to the whole system's drift. The conclusion and finding is of great significance for guiding the resources allocation for the calibration and maintenance in inertial platform system.

References

1. Hu Pinghua (2000) Study on the heading sensitive drift of inertial platform using dynamically tuned gyros. China's Carrier Rocket Technology Research Institute.
2. Nadeau F (1995) The CIGTF connection: a story of precision testing at the central inertial guidance test facility. Proceedings of the 51st Annual Meeting of the Institute of Navigation, 283-292.
3. Dong-rong Z, Bin Y (2010) Flight-test performance analysis of the platform inertial navigation system. International Symposium on Inertial Technology and Navigation, 349-354.
4. Dong-sheng W, Xiao-bin L, Yu-feng L, Ling Z, Bao-yu Z (2007) Influence of 1N alternating components of DTG's output on platform heading sensitivity. Journal of Chinese Inertial Technology 15: 44-50.

5. Fangsuo L, Decheng J, Liujing C (2002) Calibration and compensation methods for heading effect of inertial navigation platform. Tactical Missile Technology 37: 23-27.

6. Pinghua H, Zuliang D (2001) Compensation of quadrature spring rate amplifier for platform heading sensitive drift. Journal of Chinese Inertial Technology 9: 31-35.

7. Pinghua HU, Zuliang DU (2003) Effect and compensation of servo loop zero to the drift of platform heading-effect. Control Technology of Tactical Missile 42: 34-38.

8. Masayuki K, Hiroyuki O (2005) Running torque of ball bearings with polymer lubricant (running torque foumulas). Transactions of the Japan Society of Mechanical Engineering C 71: 272-279.

9. Leblance A, Nelias D (2007) Ball motion and sliding friction on a four-contact point ball bearing. Journal of Tribology 129: 801-808.

10. Chuan-tong Z, Shao-ren X, De-qing Y, Bo L, Yin-tao G (2009) State and development on research of friction torque of ball bearings. Bearing 8: 52-56.

11. Yongbing C, Bin Z (2007) Inertial navigation principle. National Defense Industry Press, Beijing 103-106.

12. Shie L (1988) Dynamically tuned gyroscope. National Defense Industry Press, 60-61.

13. Ronglin P (1990) Maneuverable Missile Inertial Components. Astronautics Press, 420-425.

14. Wang Fang, Tang Hao Study on the influence of navigation heading sensitive drift caused by servo loop zero. Flight Automatic Control Research Institute, 290-293.

15. Szuminski P, Kapitaniak T (2005) A Model for the determination of the resisting torque of the rolling bearing cage motion of slow-speed kinematic pairs. Meccanica 40: 35-47

16. Mengsu L (2008) Friction moment analysis of bearings in small power unit system of bali-pen machine with multi-station. Journal of Donghua University 34: 471-474.

17. Jianghong Z (2000) The research of the friction moment of low speed ball bearing. Missiles and Space Vehicles 248: 20-25.

18. Lun-dong Z, Xian-fei P, Mei-ping W (2006) Design and analysis of pre-amplifier for detection circuit of mechanically dithered ring laser gyroscope. Optoelectronic Technology 26: 110-114.

19. Chaowu J, Longxiang X (2009) Measurement error of displacement sensors for active magnetic bearings. Journal of Nanjing University of Aeronautics & Astronautics 41: 627-632.

20. Fuqiang G (1995) Inertial platform of the induced vibration drift. Journal of Northwestern Polytechnical University 13: 92-97.